

Giant magnetocaloric effect in Ho₁₂Co₇ compound

X. Q. Zheng, X. P. Shao, J. Chen, Z. Y. Xu, F. X. Hu et al.

Citation: *Appl. Phys. Lett.* **102**, 022421 (2013); doi: 10.1063/1.4788706

View online: <http://dx.doi.org/10.1063/1.4788706>

View Table of Contents: <http://apl.aip.org/resource/1/APPLAB/v102/i2>

Published by the [American Institute of Physics](#).

Related Articles

Magnetic properties and magnetocaloric effects in Er_{3-x}GdxCo intermetallic compounds
J. Appl. Phys. **113**, 033908 (2013)

Giant magnetocaloric and barocaloric effects in R₅Si₂Ge₂ (R=Tb, Gd)
J. Appl. Phys. **113**, 033910 (2013)

Giant low field magnetocaloric effect in soft ferromagnetic ErRuSi
Appl. Phys. Lett. **102**, 022408 (2013)

Low-temperature large magnetocaloric effect in the antiferromagnetic ErNi_{0.6}Cu_{0.4}Al compound
J. Appl. Phys. **113**, 023916 (2013)

Effect of hydrostatic pressure on magnetic entropy change and critical behavior of the perovskite manganite La_{0.4}Bi_{0.3}Sr_{0.3}MnO₃
J. Appl. Phys. **113**, 023904 (2013)

Additional information on *Appl. Phys. Lett.*

Journal Homepage: <http://apl.aip.org/>

Journal Information: http://apl.aip.org/about/about_the_journal

Top downloads: http://apl.aip.org/features/most_downloaded

Information for Authors: <http://apl.aip.org/authors>

ADVERTISEMENT

AIP | Applied Physics
Letters

SURFACES AND INTERFACES
Focusing on physical, chemical, biological, structural, optical, magnetic and electrical properties of surfaces and interfaces, and more...

ENERGY CONVERSION AND STORAGE
Focusing on all aspects of static and dynamic energy conversion, energy storage, photovoltaics, solar fuels, batteries, capacitors, thermoelectrics, and more...

EXPLORE WHAT'S NEW IN APL

SUBMIT YOUR PAPER NOW!

Giant magnetocaloric effect in Ho₁₂Co₇ compound

X. Q. Zheng,¹ X. P. Shao,¹ J. Chen,² Z. Y. Xu,¹ F. X. Hu,¹ J. R. Sun,¹ and B. G. Shen^{1,a)}

¹State Key Laboratory for Magnetism, Institute of Physics, Chinese Academy of Sciences, Beijing 100190, People's Republic of China

²Beijing Institute of Aerospace Testing Technology, China Aerospace Science and Technology Corporation, Beijing 100074, People's Republic of China

(Received 15 October 2012; accepted 7 January 2013; published online 18 January 2013)

Magnetic properties and magnetocaloric effects of Ho₁₂Co₇ compound are investigated by magnetization and heat capacity measurement. The Ho₁₂Co₇ compound undergoes antiferromagnetic (AFM)-AFM transition at $T_1 = 9$ K, AFM-ferromagnetic (FM) transition at $T_2 = 17$ K, and FM-paramagnetic transition at $T_C = 30$ K, with temperature increasing. There are two peaks on the magnetic entropy change (ΔS_M) versus temperature curves and the maximal value of $-\Delta S_M$ is found to be 19.2 J/kg K with the refrigerant capacity value of 554.4 J/kg under a field change from 0 to 5 T. The shape of the ΔS_M - T curves obtained from heat capacity measurement is in accordance with that from magnetization measurement. The excellent magnetocaloric performance indicates the applicability of Ho₁₂Co₇ as an appropriate candidate for magnetic refrigerant in low temperature ranges. © 2013 American Institute of Physics. [<http://dx.doi.org/10.1063/1.4788706>]

Magnetic refrigeration based on magnetocaloric effect (MCE) is a kind of technology used for cooling and it has several advantages such as environment friendliness and high efficiency compared with gas compression-expansion refrigeration.¹⁻⁴ Many magnetic materials with first-order phase transition have been found to exhibit large MCEs, such as Gd₅Si₂Ge₂, La(Fe,Si)₁₃, MnAs_{1-x}Sb_x, MnFeP_{1-x}As_x, and NiMnGa.⁵⁻¹⁰ Much attention has also been paid to the rare earth (R)-based intermetallic compounds with a giant MCE and low-temperature phase transition for the purpose of magnetic refrigerant application.¹¹⁻¹³ Especially, the materials with two or more transitions exhibit considerable value of refrigerant capacity (RC), because all the transitions contribute to the magnetic entropy change (ΔS_M).¹⁴⁻¹⁷

It was reported that there are eight intermetallic compounds existing in the Co-Ho system, and Ho₁₂Co₇ is among them.¹⁸ Although R₁₂Co₇ (R = Gd, Tb, Dy, Ho, Er) compounds have identical monoclinic structures, they exhibit different magnetic properties.¹⁹ Both of Gd₁₂Co₇ and Tb₁₂Co₇ compounds undergo one ferromagnetic (FM)-paramagnetic (PM) transition and the maximal values of magnetic entropy change ($-\Delta S_M$) are observed to be 4.6 and 3.08 J/kg K for a field change of 0-2 T, respectively.^{20,21} However, a spin reorientation behavior, with no contribution to MCE, is observed below Curie temperature (T_C) for the Gd₁₂Co₇ compound.²²

In the present paper, the magnetic properties and MCEs of Ho₁₂Co₇ compound are investigated by magnetization and heat capacity measurement. Two peaks close to each other are observed on the curves of ΔS_M versus temperature. The maximal $-\Delta S_M$ and RC values are found to be 9.2 J/kg K and 206.2 J/kg for a field change of 0-2 T, respectively. And as for a field change of 0-5 T, the maximal $-\Delta S_M$ and RC values are found to be 19.2 J/kg K and 554.4 J/kg, respectively.

Polycrystalline Ho₁₂Co₇ was prepared by arc melting starting materials in a high-purity argon atmosphere. The

purities of starting materials were better than 99.9%. The sample was turned over and remelted several times to ensure its homogeneity. Ingot obtained by arc melting was subsequently wrapped by molybdenum foil, sealed in a quartz tube of high vacuum, annealed at 1023 K for 7 days, and then quenched to room temperature. The crystal structure of the samples was characterized using x-ray powder diffraction (XRD) using Cu K α radiation. Magnetizations were measured as functions of both temperature and magnetic field by using a vibrating sample magnetometer with quantum design (SQUID-VSM). Heat capacity measurements were carried out by employing Physical Properties Measurement System (PPMS).

The room-temperature powder XRD pattern of Ho₁₂Co₇ is shown in Fig. 1. Almost all of the diffraction peaks can be indexed to a monoclinic crystal structure (space group $P2_1/c$). The lattice parameters are determined to be $a = 8.325(1)$, $b = 11.134(3)$, $c = 13.769(4)$ by using the Rietveld refinement method, which is very close to those reported in Ref. 19. The Rietveld refinement result also shows that a small amount of HoCo₃ exists. Anyway, they do not affect our discussions and conclusions on the Ho₁₂Co₇ compound.

The temperature (T) dependence of magnetization (M) was measured in both zero field-cooled (ZFC) and field-cooled (FC) processes in order to determine the thermal hysteresis and the magnetic transition temperature. Figure 2(a) shows the thermomagnetic M - T curves of Ho₁₂Co₇ measured under an external magnetic field of 0.01 T. According to the M versus T characteristics, it is suggested that the Ho₁₂Co₇ compound undergoes three magnetic transitions in sequence with decreasing temperature. The transition at the highest temperature corresponds to a change from PM-to-FM state at $T_C = 30$ K. The rest two phase transitions are FM-antiferromagnetic (AFM) transition at $T_2 = 17$ K and AFM-AFM transition at $T_1 = 9$ K, which will be confirmed by the isothermal magnetization curves.

The M - T curves under different external magnetic field are shown in Fig. 2(b). One can find that T_1 increases

^{a)}Electronic mail: shenbg@iphy.ac.cn.

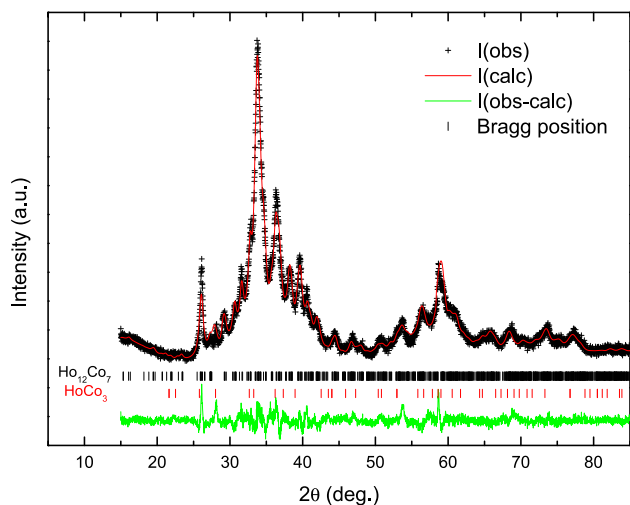


FIG. 1. Rietveld refined powder x-ray diffraction pattern of $\text{Ho}_{12}\text{Co}_7$ at room temperature. The observed data are indicated by crosses and the calculated profile is the continuous line overlaying them. The short vertical lines indicate the angular positions of the Bragg peaks of $\text{Ho}_{12}\text{Co}_7$. The lower curve is the difference between the observed and calculated intensity.

monotonically with magnetic field increasing from 0.01 to 0.3 T. However, almost no change is observed for T_2 and T_C with magnetic field change. It indicates that a field-induced metamagnetic transition from AFM to FM state occurs below T_2 , and T_1 is pushed towards higher temperature with the applied magnetic field increasing. Similar phenomenon has been observed in PrGa compound.²³

The temperature dependences of the heat capacity in different magnetic fields are shown in Fig. 2(c). The peaks

around 30 K, which are obvious for $H=0$ T and 0.5 T, are corresponding to T_C . It is found that there are obvious differences of heat capacity below T_2 for different magnetic field. The reason why the applied magnetic field affects heat capacity so greatly is that a magnetic transition from the weak AFM ground state to the FM state occurs. There is no obvious peak related to AFM-AFM transition temperature for zero-field heat capacity curve, but a clear peak around 13 K appears on the heat capacity curve for an applied field of 0.5 T. As is illustrated in the M - T curves, the peak is corresponding to AFM-AFM transition and it has been pushed by the applied field from T_1 ($=9$ K) to higher temperature (~ 13 K). In the temperature range between T_2 and T_C , the differences of heat capacity for different magnetic field are not as clear as those in lower temperature range. That is because $\text{Ho}_{12}\text{Co}_7$ compound is FM state in this range, and the influence of applied field on heat capacity is small. The heat capacity data demonstrate that the statement of magnetic transition on the basis of M - T curves is reasonable.

It is also found from Fig. 2(a) that the heating and cooling M - T curves show a reversible behavior near T_C and it is accompanied without thermal hysteresis, indicating a nature of the second-order phase transition. The inset of Fig. 2(a) shows the reciprocal magnetic susceptibility χ^{-1} versus temperature. It is found that the magnetic susceptibility of the $\text{Ho}_{12}\text{Co}_7$ compound can be fitted to the Curie-Weiss law above ~ 40 K. The effective magnetic moment μ_{eff} per Ho ion for $\text{Ho}_{12}\text{Co}_7$, obtained from the linear temperature dependence of χ^{-1} , is $11.3 \mu_B$, which is close to the value expected for a free Ho^{3+} ion ($\mu_{\text{eff}} = 10.6 \mu_B$). Considering

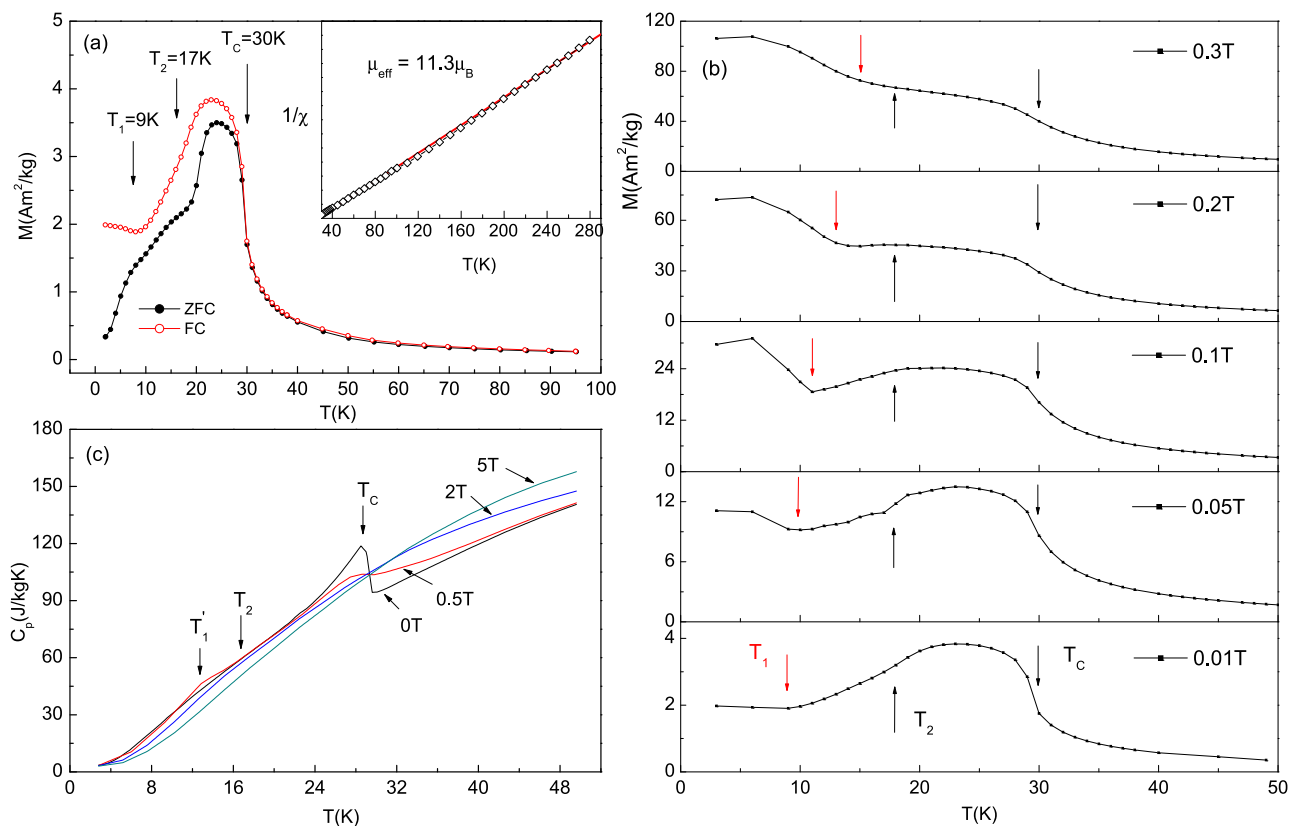


FIG. 2. (a) Temperature dependences of ZFC and FC magnetization for $\text{Ho}_{12}\text{Co}_7$ under a magnetic field of 0.1 T and the inset shows the reciprocal magnetic susceptibility χ^{-1} versus temperature. (b) Temperature dependences of magnetizations for $\text{Ho}_{12}\text{Co}_7$ under different magnetic field. (c) Temperature dependences of heat capacity for different magnetic field.

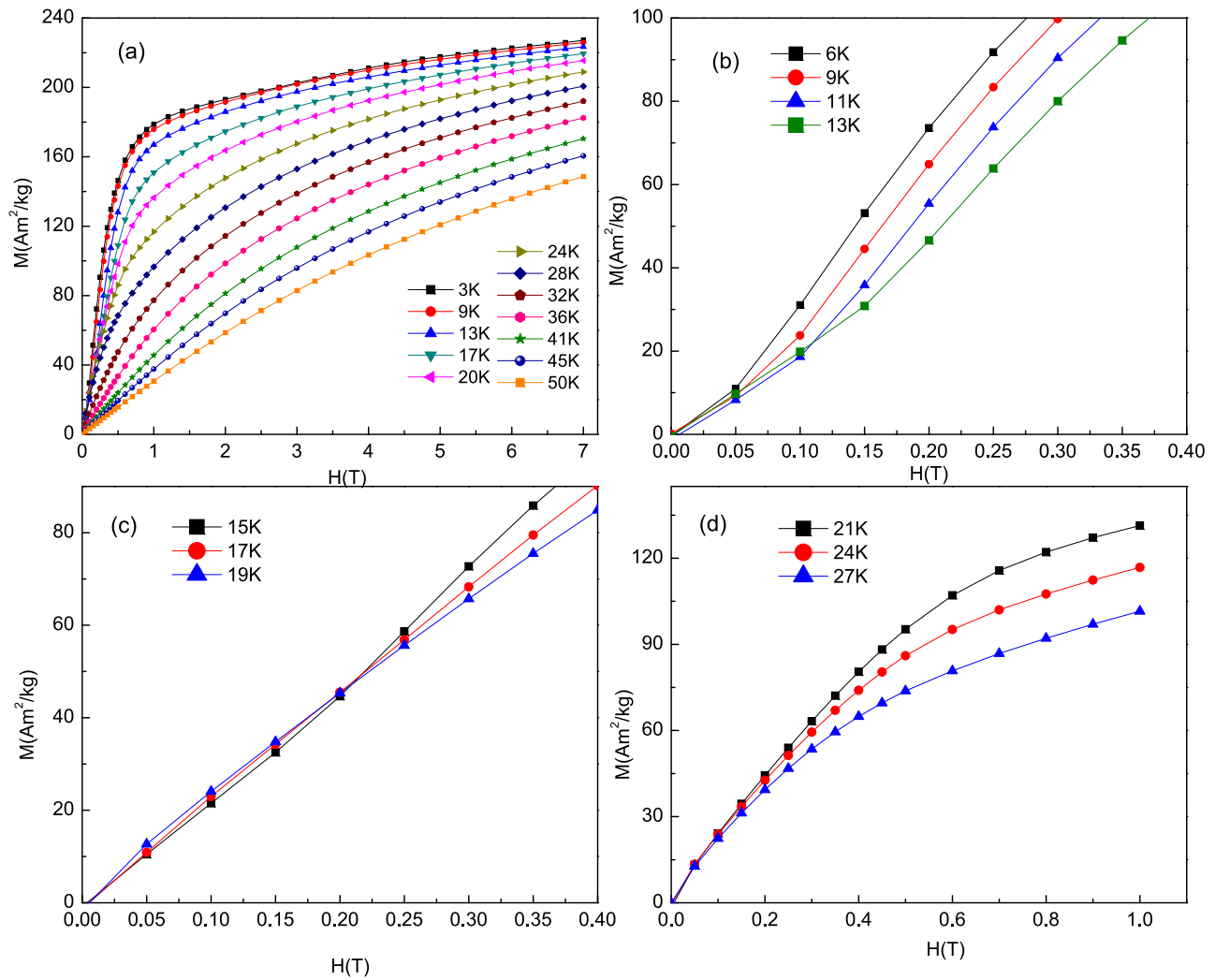


FIG. 3. (a) Magnetic isothermals of $\text{Ho}_{12}\text{Co}_7$ in the temperature range of 3–50 K. (b) Magnetic isothermals in the low magnetic field region at 6 K, 9 K, 11 K, and 13 K. (c) Magnetic isothermals in the low magnetic field region at 15 K, 17 K, and 19 K. (d) Magnetic isothermals in the low magnetic field region at 21 K, 24 K, and 27 K.

that the sample is almost a single phase and free from impurities, the small difference may result from a small moment on Co as observed in $\text{Tb}_6\text{Co}_{1.67}\text{Si}_3$.²⁴

Figure 3(a) shows the isothermal magnetization curves of $\text{Ho}_{12}\text{Co}_7$ in a temperature range of 3–50 K under the magnetic fields up to 7 T. The isothermal magnetization curves in some selected temperature ranges at low magnetic fields are shown in Figs. 3(b)–3(d), respectively. One can find that the isothermal magnetization curves between $T_2 = 17$ K and $T_C = 30$ K show FM characters (Fig. 3(d)). The magnetization remains a linear dependence of the magnetic field at low field range below $T_2 = 17$ K (Figs. 3(b) and 3(c)), indicating the existence of AFM ground state. Now we can confirm the transition around T_2 is corresponding to FM-AFM transition, and the one around T_1 is corresponding to AFM-AFM transition. The magnetization curves deviate from the linear relationship, when the applied field exceeds a certain value, showing a field-induced metamagnetic transition from AFM to FM state. The critical field determined from the maximum of dM/dH for $\text{Ho}_{12}\text{Co}_7$ is found to be 0.12 T at 6 K and 0.28 T at 16 K. The result indicates that the $\text{Ho}_{12}\text{Co}_7$ compound is a weak antiferromagnet below T_2 , and a small magnetic field can destroy the AFM structure. One can also

find from Fig. 3(a) that the isothermal magnetization curves obtained well above T_C show strong curvatures at low fields. Similar results have been observed in some other intermetallic compounds.^{14,25,26} It may result from the existence of short-range ferromagnetic correlations in the PM state. The Arrott plot of $\text{Ho}_{12}\text{Co}_7$ is shown in Fig. 4. In the Landau free energy theory, an S-shaped curve is expected when there is a

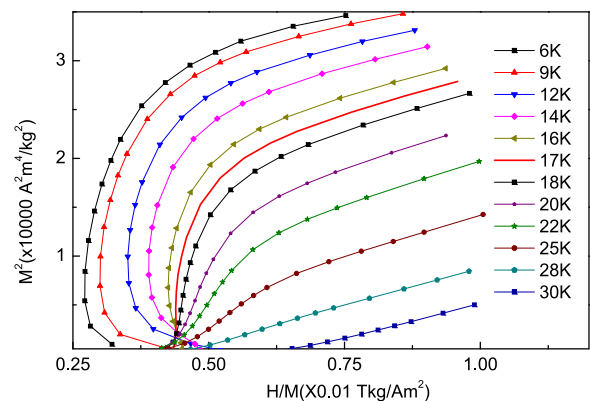


FIG. 4. Arrott plot of $\text{Ho}_{12}\text{Co}_7$ in a temperature range of 6–33 K with the temperature step of 2 K or 3 K.

negative contribution of some higher order term, such as a negative M^4 -term, in the Landau free energy expansion. And the appearance of S-shaped Arrott plots can be used to affirm the occurrence of metamagnetism transition.²⁷ The S-shaped Arrott plots below T_2 confirm the existence of the field-induced first-order AFM-FM transition. The positive slope of the Arrott plot above T_C indicates a characteristic of a second-order PM-FM transition.

The ΔS_M of $\text{Ho}_{12}\text{Co}_7$ was calculated from isothermal magnetization data by using the Maxwell relation $\Delta S_M = \int_0^H (\partial M / \partial T)_H dH$ and from heat capacity data through the expression $\Delta S_M = \int_0^H \{ [C(T, H) - C(T, 0)] / T \} dT$ as well.²⁸ Figure 5(a) shows the ΔS_M as a function of temperature for different magnetic field changes. The curves obtained using magnetization data are not in good agreement with the corresponding curves obtained using heat capacity. Considering that the actual combined relative error in the ΔS_M calculated from magnetization data can reach $\sim 20\%$ and that from heat capacity data can be $\sim 4\%$,^{28,29} the deviations between the value of ΔS_M calculated from the two methods are in the error range with the maximal error being $\sim 17\%$ and $\sim 11\%$, for the field change of 0-2 T and 0-5 T, respectively. Although there are differences between the curves obtained from the two methods, the shape of the curves matches well with each other. It is clear that there are two peaks on the ΔS_M - T curves, which indicates that both AFM-FM and PM-FM transitions contribute to MCE. Figure 5(b) shows that when the field change is small, for example, 0-0.2 T, the value of ΔS_M is positive in certain temperature range, and as the field change

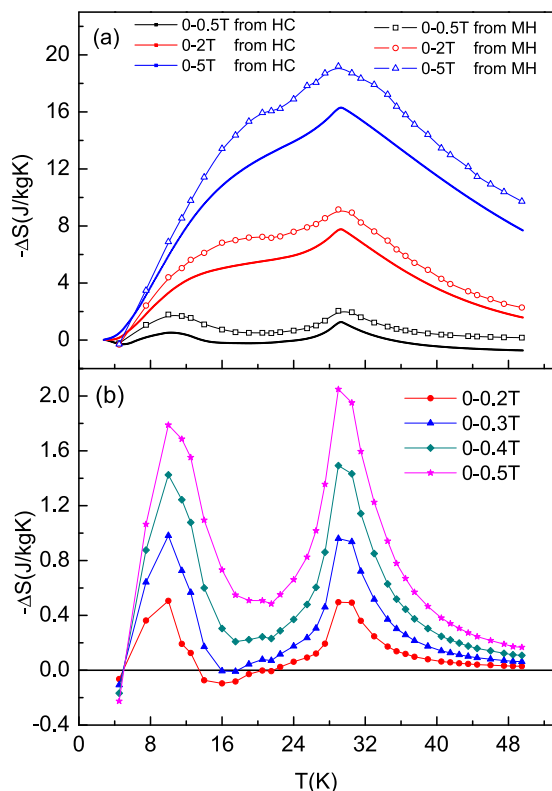


FIG. 5. (a) Temperature dependences of magnetic entropy change (ΔS_M) calculated from magnetization and heat capacity data for field changes of 0-0.5 T, 0-2 T, and 0-5 T, respectively. (b) Temperature dependences of magnetic entropy change (ΔS_M) calculated from magnetization only for field changes of 0-0.2 T, 0-0.3 T, 0-0.4 T, and 0-0.5 T, respectively.

increasing, the value of ΔS_M changes into negative. That results from the occurrence of metamagnetism transition, because the positive or negative value of ΔS_M is related to AFM or FM state. Besides, with the field change increasing, the first peak corresponding to AFM-FM transition moves towards higher temperatures, while the second peak related to PM-FM transition almost centers at ~ 30 K, which is in accordance with the results of M - T and C_p - T measurement. When the field change is high enough, for example, 0-2 T and 0-5 T, the first peak is so close to the second one that they almost change into a larger peak. On the basis of magnetization measurement, the maximal value of $-\Delta S_M$ for $\text{Ho}_{12}\text{Co}_7$ is found to be 19.2 J/kg K around T_C for a field change 0-5 T. Compared with the refrigerant materials in a similar temperature range, the value of $\text{Ho}_{12}\text{Co}_7$ compound is smaller than that of ErGa (21.3 J/kg K at 30 K),¹⁴ DyCuAl (20.4 J/kg K at 28 K),³⁰ and ErCo₂ (33 J/kg K at 36 K)³¹ compounds, but it is larger than that of DyNiAl (19 J/kg K at 32 K),³² TbCoC₂ (15.3 J/kg K at 30 K),³³ and GdNi₅ (11.5 J/kg K at 32 K).³⁴

One can also see from Fig. 5(a) that both the peak value and peak width of ΔS_M - T curves depend on the magnetic field change. When the field change is 0-0.5 T, the maximum value of the two peaks is small and they are far apart from each other. However, when the applied field increases to 2 T and 5 T, the two peaks become one larger peak. That is to say, both of the maximal value and the width of the peak have an obvious increase. The peak shape is very helpful to improvement of the value of RC in $\text{Ho}_{12}\text{Co}_7$ compound. The RC value of $\text{Ho}_{12}\text{Co}_7$ compound was also calculated by using the approach suggested by Gschneidner *et al.*³⁵ The RC is defined as $RC = \int_{T_1}^{T_2} |\Delta S_M| dT$, where T_1 and T_2 are the temperatures corresponding to both sides of the half-maximum value of ΔS_M peak, respectively. The RC value of $\text{Ho}_{12}\text{Co}_7$ is estimated to be 206.2 J/kg with $T_1 = 10.4$ K (temperature of the cold reservoir) and $T_2 = 39.8$ K (temperature of the hot reservoir) for a field changing from 0 to 2 T. And the RC value is estimated to be 554.9 J/kg with $T_1 = 12.3$ K and $T_2 = 49.8$ K for a field changing from 0 to 5 T. As a result, $\text{Ho}_{12}\text{Co}_7$ compound has an outstanding refrigerant capacity among the magnetocaloric materials in a similar temperature range, such as ErGa (RC = 494 J/kg with $T_1 = 14.3$ K and $T_2 = 45.2$ K),¹⁴ DyCuAl (RC = 427 J/kg with $T_1 = 17$ K and $T_2 = 45$ K),³⁰ ErCo₂ (RC = 273 J/kg with $T_1 = 33$ K and $T_2 = 43$ K),³¹ DyNiAl (RC = 492 J/kg with $T_1 = 19$ K and $T_2 = 53$ K),³² TbCoC₂ (RC = 354 J/kg with $T_1 = 23.5$ K and $T_2 = 50$ K)³³ and GdNi₅ (RC = 198 J/kg with $T_1 = 21$ K and $T_2 = 45$ K),³⁴ although ErGa, DyCuAl, and ErCo₂ exhibit larger ΔS_M values. Here, the RC values of some compounds are estimated from the temperature dependence of ΔS_M in the literatures, respectively. The large value of ΔS_M and RC suggests that $\text{Ho}_{12}\text{Co}_7$ can be an appropriate candidate for magnetic refrigerant in low temperature ranges.

In summary, the $\text{Ho}_{12}\text{Co}_7$ compound undergoes a PM-FM transition at $T_C = 30$ K, accompanied with a FM-AFM transition at $T_2 = 17$ K and an AFM-AFM transition at $T_1 = 9$ K. A field-induced metamagnetic transition from AFM to FM state occurs below T_2 . With the magnetic field increasing, T_1 moves towards higher temperatures, but T_2 and T_C almost keep the same value. There are two peaks on the ΔS_M - T curves and they become one larger peak when the

field change is 0–2 T and 0–5 T. The maximal values of $-\Delta S_M$ and RC are determined to be 19.2 J/kg K and 554.9 J/kg for a field change of 0–5 T, respectively. The large value of ΔS_M and RC suggests that $\text{Ho}_{12}\text{Co}_7$ can be an appropriate candidate for magnetic refrigerant in low temperature ranges.

This work was supported by the National Natural Science Foundation of China, the Hi-Tech Research and Development program of China, the Key Research Program of the Chinese Academy of Sciences, and the National Basic Research of China.

- ¹K. A. Gschneidner, Jr., V. K. Pecharsky, and A. O. Tsokol, *Rep. Prog. Phys.* **68**, 1479 (2005).
- ²E. Brück, in *Handbook of Magnetic Materials*, edited by K. H. J. Buschow (Elsevier B. V., 2008), Vol. 17, p. 235.
- ³B. G. Shen, J. R. Sun, F. X. Hu, H. W. Zhang, and Z. H. Chen, *Adv. Mater.* **21**, 4545 (2009).
- ⁴V. K. Pecharsky and K. A. Gschneidner, Jr., *Annu. Rev. Mater. Sci.* **30**, 387 (2000).
- ⁵V. K. Pecharsky and K. A. Gschneidner, Jr., *Phys. Rev. Lett.* **78**, 4494 (1997).
- ⁶F. X. Hu, B. G. Shen, J. R. Sun, Z. H. Chen, G. H. Rao, and X. X. Zhang, *Appl. Phys. Lett.* **78**, 3675 (2001).
- ⁷H. Wada and Y. Tanabe, *Appl. Phys. Lett.* **79**, 3302 (2001).
- ⁸O. Tegus, E. Brück, K. H. J. Buschow, and F. R. de Boer, *Nature (London)* **415**, 150 (2002).
- ⁹F. X. Hu, B. G. Shen, and J. R. Sun, *Appl. Phys. Lett.* **76**, 3460 (2000).
- ¹⁰F. X. Hu, B. G. Shen, J. R. Sun, and G. H. Wu, *Phys. Rev. B* **64**, 132412 (2001).
- ¹¹J. Shen, F. Wang, Y. X. Li, J. R. Sun, and B. G. Shen, *J. Alloys Compd.* **458**, L6 (2008).
- ¹²B. Li, J. Du, W. J. Ren, W. J. Hu, Q. Zhang, D. Li, and Z. D. Zhang, *Appl. Phys. Lett.* **92**, 242504 (2008).
- ¹³P. Kumar, K. G. Suresh, and A. K. Nigam, *J. Phys. D: Appl. Phys.* **41**, 105007 (2008).
- ¹⁴J. Chen, B. G. Shen, Q. Y. Dong, F. X. Hu, and J. R. Sun, *Appl. Phys. Lett.* **95**, 132504 (2009).
- ¹⁵J. Chen, B. G. Shen, Q. Y. Dong, and J. R. Sun, *Solid State Commun.* **150**, 157 (2010).
- ¹⁶X. Q. Zheng, J. Chen, J. Shen, H. Zhang, Z. Y. Xu, W. W. Gao, J. F. Wu, F. X. Hu, J. R. Sun, and B. G. Shen, *J. Appl. Phys.* **111**, 07A917 (2012).
- ¹⁷J. Shen, J. L. Zhao, F. X. Hu, G. H. Rao, G. Y. Liu, J. F. Wu, Y. X. Li, J. R. Sun, and B. G. Shen, *Appl. Phys. A* **99**, 853 (2010).
- ¹⁸K. H. J. Buschow, *Philips Res. Rep.* **26**, 49–64 (1971).
- ¹⁹W. Adams, J. M. Moreau, E. Parthé, and J. Schweizer, *Acta Crystallogr. B* **32**, 2697 (1976).
- ²⁰X. Chen and Y. H. Zhuang, *Solid State Commun.* **148**, 322 (2008).
- ²¹J. Q. Deng, Y. H. Zhuang, J. Q. Li, and J. L. Huang, *Physica B* **391**, 331 (2007).
- ²²Z. G. Zhong, X. C. Zhong, H. Y. Yu, Z. W. Liu, and D. C. Zeng, *J. Appl. Phys.* **109**, 07A919 (2011).
- ²³J. Chen, X. Q. Zheng, Q. Y. Dong, J. R. Sun, and B. G. Shen, *Appl. Phys. Lett.* **99**, 122503 (2011).
- ²⁴A. Haldar, N. K. Singh, K. G. Suresh, and A. K. Nigam, *Physica B* **405**, 3446 (2010).
- ²⁵R. Mallik, E. V. Sampathkumaran, and P. L. Paulose, *Solid State Commun.* **106**, 169 (1998).
- ²⁶P. Arora, P. Tiwari, V. G. Sathe, and M. K. Chattopadhyay, *J. Magn. Magn. Mater.* **321**, 3278 (2009).
- ²⁷N. H. Duc, D. T. Anh, and P. E. Brommer, *Physica B* **319**, 1 (2002).
- ²⁸V. K. Pecharsky and K. A. Gschneidner, Jr., *J. Appl. Phys.* **86**, 565 (1999).
- ²⁹V. K. Pecharsky and K. A. Gschneidner, Jr., *J. Magn. Magn. Mater.* **200**, 44 (1999).
- ³⁰Q. Y. Dong, B. G. Shen, J. Chen, J. Shen, and J. R. Sun, *J. Appl. Phys.* **105**, 113902 (2009).
- ³¹N. K. Singh, P. Kumar, K. G. Suresh, A. K. Nigam, A. A. Coelho, and S. Gama, *J. Phys.: Condens. Matter* **19**, 036213 (2007).
- ³²N. K. Singh and K. G. Suresh, *J. Appl. Phys.* **99**, 08K904 (2006).
- ³³B. Li, W. J. Hu, X. G. Liu, F. Yang, W. J. Ren, X. G. Zhao, and Z. D. Zhang, *Appl. Phys. Lett.* **92**, 242508 (2008).
- ³⁴P. J. von Ranke, M. A. Mota, D. F. Grangeia, A. M. G. Carvalho, F. C. G. Gandra, A. A. Coelho, A. Caldas, N. A. de Oliveira, and S. Gama, *Phys. Rev. B* **70**, 134428 (2004).
- ³⁵K. A. Gschneidner, Jr., V. K. Pecharsky, A. O. Pecharsky, and C. B. Zimm, *Mater. Sci. Forum* **315–317**, 69 (1999).